Science of the Total Environment 493 (2014) 1–11

Contents lists available at ScienceDirect

Science of the Total Environment

journal homepage: www.elsevier.com/locate/scitotenv

The importance of atmospheric base cation deposition for preventing soil acidification in the Athabasca Oil Sands Region of Canada

Shaun A. Watmough [a,*], Colin J. Whitfield [b], Mark E. Fenn [c]

[a] Environmental Resource Studies Program, Trent University, Peterborough, ON, K9J 7B8, Canada
[b] Centre for Hydrology, Geography and Planning, University of Saskatchewan, Saskatoon, SK, S7N 5C8, Canada
[c] Research Plant Pathologist, Ecosystem Function and Health Program, USDA Forest Service, Pacific Southwest Research Station, Riverside, CA 92507, United States

HIGHLIGHTS

- Base cation weathering rates in the Athabasca Oil Sands Region are very low.
- Acid deposition is greatly elevated but decreases with distance from the mines.
- Deposition of calcium and magnesium mostly exceeds sulfur deposition.
- High levels of base cation deposition mitigate potential soil acidification.

ARTICLE INFO

Article history:
Received 31 March 2014
Received in revised form 13 May 2014
Accepted 24 May 2014
Available online 14 June 2014

Editor: C.E.W. Steinberg

Keywords:
Acid deposition
Base cations
Oil sands
Mineral weathering

ABSTRACT

Industrial activities in the oil sands region of Alberta, Canada have resulted in greatly elevated emissions of SO_2 and N (NO_x and NH_3) and there are concerns over possible widespread ecosystem acidification. Acid sensitive soils in the region are common and have very low base cation weathering rates: the median base cation weathering rate estimated for 63 sites using PROFILE was just 17 $mmol_c\ m^{-2}\ yr^{-1}$. Deposition of S and N in throughfall was approximately twice as high as deposition measured with open collectors and could be as high as 360 $mmol_c\ m^{-2}\ yr^{-1}$ within 20 km of the main industrial center, although deposition declined logarithmically with distance from the industrial activities. Base cation deposition however, mostly exceeded the combined inputs of S and N in bulk deposition and throughfall, particularly during the summer months. The potential for soil acidification at a site close (<3 km) to the largest mine was assessed using the dynamic ecosystem acidification model, MAGIC (Model of Acidification of Groundwater in Catchments). Despite very low base cation weathering rates (~6 $mmol_c\ m^{-2}\ yr^{-1}$) and high (~250 $mmol_c\ m^{-2}\ yr^{-1}$) acid (S + N) deposition at the site, soil base saturation and soil solution pH and molar Ca:Al ratio were predicted to increase in the future assuming acid and base cation deposition constant at current rates. This work shows that despite extremely low soil base cation weathering rates in the region, the risk of soil acidification is mitigated to a large extent by high base cation deposition, which in contrast to S emissions is derived from fugitive dust sources in the mines, and is poorly quantified for regional modeling studies.

1. Introduction

The oil sands of Alberta, Canada are the largest oil deposit in North America, and second largest recoverable deposit in the world, with the bulk of the oil (130 billion barrels) located in the Athabasca Oil Sands Region (AOSR). Current production from oil sands is 1.6 million bbl day^{-1} (barrels per day) and production is expected to increase to 3.7 million bbl day^{-1} by 2025 (Stringham, 2012). Elevated emissions of sulfur (S) and nitrogen (N) are associated with these mining and upgrading activities; over the period 2003–2008, SO_2 emissions ranged between 274 and 314 tons day^{-1} and NO_x emissions have increased from 148 to 200 tons day^{-1} over the same period (Percy, 2013). High levels of S and N deposition can result in soil acidification leading to declines in tree health and other adverse ecological effects (Cronan and Grigal, 1995; Nellemann and Thomsen, 2001). To address concerns over potential ecosystem acidification, emissions controls for the region are regulated by an effects-based management framework based on both observed changes in mineral soil base saturation (BS) and molar base cation (BC:calcium (Ca^{2+}) + magnesium (Mg^{2+}) + potassium (K^+) + sodium (Na^+)) to aluminum ratio (BC:Al) in soil solution at monitoring plots, and model predictions of future change in these parameters (Whitfield et al., 2009).

* Corresponding author.

http://dx.doi.org/10.1016/j.scitotenv.2014.05.110
0048-9697/

The upland terrain in the AOSR has been characterized as having soils with low exchangeable base cations and low cation exchange capacity that are sensitive to acid deposition (Holowaychuk and Fessenden, 1987; Turchenek et al., 1987; Whitfield et al., 2010a, 2010b). Whitfield et al. (2010a) estimated critical loads for acid deposition for 333 sites in the region and reported that under conditions of complete N retention, 34% of the sites receive acid deposition in excess of their critical load; if all N deposition is leached, 62% of the sites are currently exceeded. The high sensitivity of these soils to acid deposition is due to the very low base cation weathering rates associated with the sandy soils (Whitfield et al., 2011), although weathering rate estimations are typically associated with considerable uncertainty (Hodson et al., 1996; Klaminder et al., 2011). There are very few long-term monitoring data that can be used to assess model predictions, but the few studies that do exist indicate that soils and lakes are not currently acidifying, and in fact soils may be becoming less acidic (Hazewinkel et al., 2008; Jung et al., 2013) suggesting model predictions are wrong or other factors are not being adequately considered.

In a recent study, Landis et al. (2012) used the chemistry of the epiphytic lichen (*Hypogymnia physodes*) at 121 sites around the AOSR to elucidate the sources and spatial distribution of inorganic air pollutants. Landis et al. (2012) identified five sources that significantly contribute to element concentrations in lichen tissue; combustion processes, tailing sand, haul roads, processed materials and a general anthropogenic urban source. Calcium concentrations in the haul road dust were >25,000 μg g^{-1}, but in contrast to emissions from stacks, dust emissions from mines are poorly quantified and not included in atmospheric deposition models (Davies, 2012). In other regions, atmospheric base cation deposition has been shown to reduce the risk of soil acidification and the S:Ca^{2+} ratio in deposition was proposed as an indicator of potential risk from acid deposition (Larssen and Carmichael, 2000). High levels of base cations in deposition therefore have the potential to offset soil acidification, yet base cation deposition for the region is poorly quantified and its potential impact on the risk of soil acidification in the region has not been assessed.

In this study, base cation (BC:Ca^{2+} + Mg^{2+} + K^{+} + Na^{+}) weathering rates were estimated for 63 sites located on acid-sensitive soils distributed widely throughout the region using PROFILE (Warfvinge and Sverdrup, 1992). Additionally, atmospheric deposition of S, dissolved inorganic nitrogen (DIN:nitrate (NO_3) and ammonium (NH_4)) and base cations (Ca^{2+}, Mg^{2+}, Na^{+}) in throughfall and in open collectors were measured using ion-exchange resin (IER) columns at 19 sites located at varying distances (3–129 km) from the industrial center. One of the major stacks in the AOSR near Fort McMurray (57° 2′ 52.75″ N, 111° 36′ 55.81″ W) was used as a central marker point for the industrial emissions, as described by Proemse et al. (2012). Finally, atmospheric deposition, soil chemistry and soil solution data collected at a site close (<3 km) to the largest mine in the AOSR were used to assess the risk of soil acidification using a dynamic ecosystem acidification model (MAGIC; The Model of Acidification of Groundwater in Catchments; Cosby et al., 1985) that has been widely used in the region (Whitfield et al., 2009, 2010a, 2010b). We hypothesized that soil base cation weathering rates would be low and that deposition of S and N would be very high, particularly close to industrial sources, but the potential for soil acidification would be mitigated by high levels of BC deposition.

2. Methods

2.1. Study area

The region of northeastern Alberta surrounding the town of Fort McMurray lies in the Boreal Plains ecozone (Environment Canada, 1996; Fig. 1). The landscape in this region features prominent areas of muskeg peatland, numerous lakes and ponds, and uplands dominated by jack pine (*Pinus banksiana*) and trembling aspen (*Populus tremuloides*). Mineral soils on the uplands are generally acid-sensitive, being eluviated dystric brunisols or, less commonly, orthic gray luvisols (Agriculture and Agri-Food Canada, 1998; Abboud et al., 2002). Typical parent materials include coarse glaciofluvial and till deposits, but coarse materials of aeolian origin are also found in the region.

2.2. Regional weathering estimates

Previous studies of upland mineral soil weathering in the AOSR have employed PROFILE for base cation weathering rate estimation (Whitfield et al., 2010a, 2010b, 2011; Whitfield and Reid, 2013). Site selection procedures differed among the studies, but the dominant mineral soil series within the region and upland soils in catchments of lakes in the region with the lowest buffering capacities were generally targeted. Consistent with the approach used in the current study (described below), detailed site-specific data were used in these investigations to estimate plot-scale weathering rates, although rather than characterizing the range in rates, a single best-estimate was calculated for each of these sites (n = 63). The sites represent a broad range of upland soil characteristics for the region (e.g. Whitfield et al., 2010b); weathering rates were calculated for a standardized (average) rooting zone depth of 0.5 m. Soil surface area was estimated from texture (Whitfield et al., 2010a, 2010b, 2011) or was measured (Whitfield and Reid, 2013). Similarly, mineral content of the soils in these past studies was determined quantitatively by x-ray diffraction, rather than the oxide-based approach described below for the current study. The differences in approach to PROFILE parameterization among studies are nonetheless minor, and together these data yield a comprehensive depiction of upland forest soil base cation weathering rates for the region.

2.3. Regional deposition in throughfall and open collectors

Atmospheric deposition of inorganic N and S in throughfall under jack pine canopies and in bulk deposition in forest clearings has been measured since May 2008 at 13–16 jack pine plots in the AOSR at a subset of the Terrestrial Environmental Effects Monitoring jack pine monitoring network operated by the Wood Buffalo Environmental Association. The deposition monitoring network covers an area of ca. 34,000 km^2. For the data included in the present study deposition was measured in a total of 18 different plots (although only 13–16 simultaneously) because the plots selected for deposition monitoring evolved over time. Deposition of base cations was also measured for one year (including separate winter and summer exposure periods; October 2009 to October 2010) at a subset of the throughfall monitoring sites that includes the lysimeter site. This network of deposition monitoring sites made possible the characterization of deposition gradients for N, S and base cations in relation to distance from the main Oil Sands industrial center, and deposition data from the most distant sites over 100 km from the source area provide estimates of background level deposition (Fenn and Ross, 2010).

For the present study data on deposition of N and S at the lysimeter site are included for May 2008 to May 2011 and deposition of base cations and N + S at 19 sites, including the lysimeter site, from October 2009 to October 2010. The summer of 2010 was a low fire year in Alberta, Canada with the area burned only 40% of the long-term average from 1996 to 2012 (http://esrd.alberta.ca/wildfire/wildfire-maps/historical-wildfire-information/default.aspx). Thus we don't expect that forest fires in summer 2010 had a major effect on base cation deposition. Nor were precipitation inputs low enough during the base cation monitoring period (October 2009 to October 2010) to cause an increase in fugitive dust emissions and base cation deposition. Precipitation in winter 2009/2010 (October 1 to April 30; 174 mm) as illustrated by the Mildred Lake site was 28% higher than the average

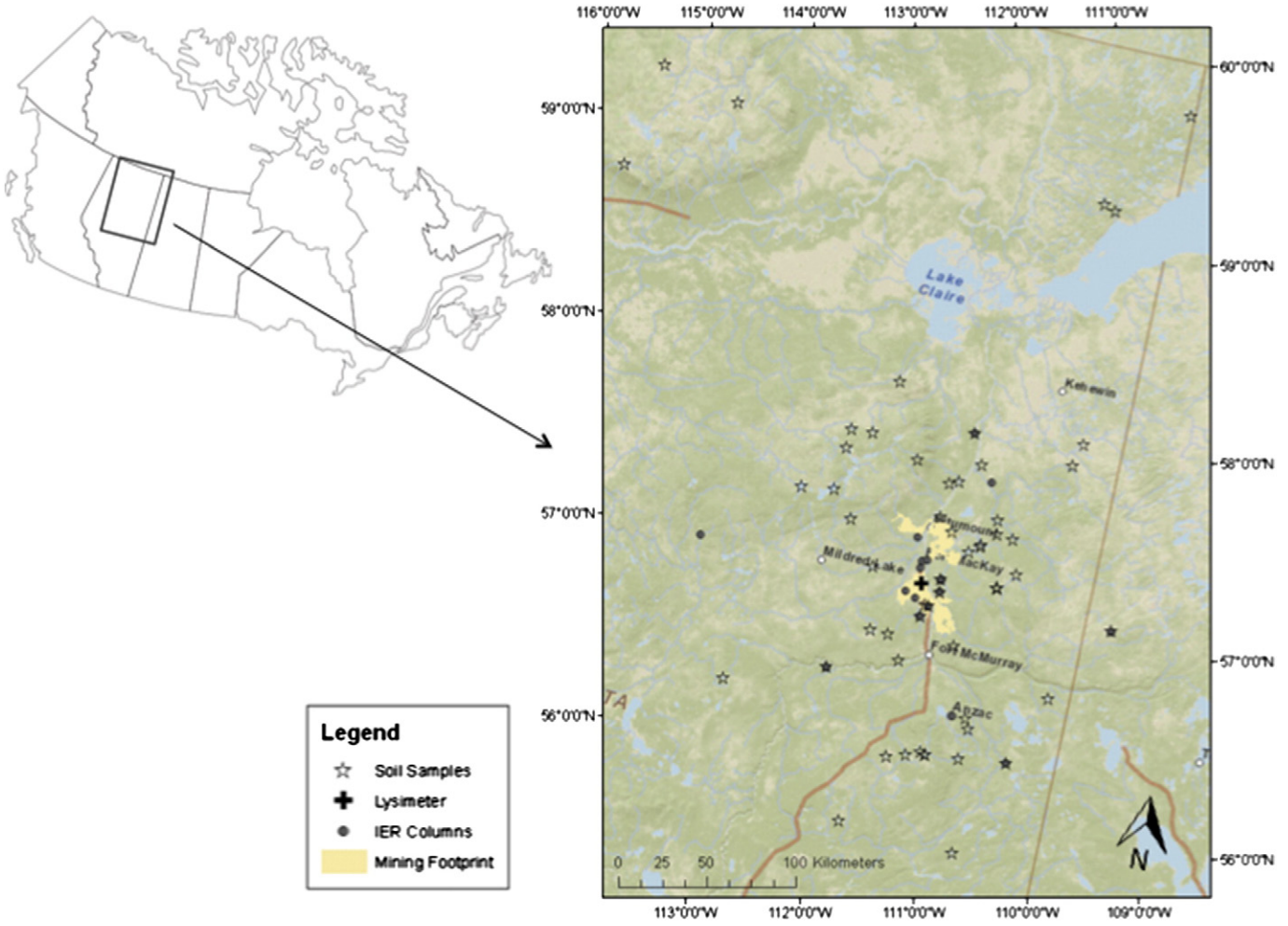

Fig. 1. Study site map of the 63 soil sample locations, 18 IER deposition monitoring locations, and the one lysimeter site.

for the 1996–2012 period. Precipitation in summer 2010 (May 1 to September 30) was near the long term average; 215 mm at Mildred Lake, only 10% below the average for 1996–2012 (http://climate.weather.gc.ca/index_e.html). When considering the four years of N and S deposition data included (May 2008 to May 2011), precipitation during summer at Mildred Lake was −20, −35, −10 and −59 percent respectively, of the long term average. The dry summer of 2011 was a high fire year, with the area burned 4 times larger than an average year. Precipitation in winter during the May 2008 to May 2011 period was −22, 28, −39 and 0 percent different respectively than the long term average.

We compared N + S deposition among the four monitoring years in order to evaluate how typical deposition was in summer 2010 and winter 2009/2010 when base cation deposition was measured. Deposition of N + S in summer 2010 was typical of the other summers except for summer 2011 when deposition to the open site collectors was low because of low rainfall. However summertime throughfall deposition was similar in all years, except summer 2008 when throughfall N + S deposition was nearly double the later years because a greater proportion of throughfall monitoring sites were located adjacent to the industrial center in 2008. In contrast, in winter 2009/2010 when base cation deposition was measured, N + S deposition was on average 65% and 231% higher in open areas and in throughfall, respectively compared to the other three years. This may have been at least partially due to greater precipitation in winter 2009/2010 compared to the other years, as mentioned above. However, greater precipitation in winter 2009/2010 may have also increased soil moisture and reduced the amount of base cations released to the atmosphere in fugitive dust during the winter base cation monitoring period.

2.4. Dynamic model predictions

2.4.1. Model description

The Model of Acidification of Groundwater in Catchments (MAGIC: Cosby et al., 1985, 2001) is a process-oriented lumped parameter dynamic hydrogeochemical model developed to investigate long-term chemical response of ecosystems to acidic deposition. The model is typically used to simulate annual surface and soil water concentrations of SO_4^{2-}, NO_3^-, Cl^-, NH_4^+, Ca^{2+}, Mg^{2+}, Na^+, K^+, Al, as well as pH and soil exchangeable base cations. Application of the model to investigate soils at the plot-scale, and independently of associated surface waters, is also possible (Whitfield et al., 2009). At the plot-scale, an aggregated uniform soil compartment is parameterized using detailed physicochemical data and information on soil processes.

The model structure is such that equilibrium reactions account for short-term processes governing ionic balance, while catchment mass balance is achieved through long-term input–output processes. Key processes include soil adsorption and exchange of base cations and Al, soil solution pH buffering by weak organic and inorganic acids, mineral weathering, and biologically mediated uptake. Rates of change for each

ion are calculated through the mass balance equations; collectively these equations describe the input–output relationships for base cations and strong acid anions in soil water. The latest version of the model, 7.77ext was used in the current study.

2.4.2. Site data

The study site (Fig. 1) is located approximately 3 km from the Syncrude mine, north of Fort McMurray in northern Alberta within an even-aged (~50 year old) jack pine stand with relatively flat topography. Soil samples from each rooting zone horizon (LFH, Ae, Bj) were collected using a trowel from the four faces of each soil pit that was dug for lysimeter installation. The soils are classified as eluviated dystric brunisols (Soil Classification Working Group, 1998) and are moderately acidic with a very high sand content with a very low cation-exchange capacity (Table 1). The long term average annual precipitation is 455 mm, of which 75% falls as rain. Fifty percent of total annual precipitation falls during the months of June, July and August. Measurement of atmospheric deposition fluxes of S and N to the site began in 2008 and continued for three years; base cation deposition (Ca^{2+}, Mg^{2+}, Na^{+}) was observed over a 12 month period in 2009–2010.

2.4.3. Soil

Stainless steel tension lysimeters (Soil Measurement Systems) were installed at a depth of 0.25 m from the top of the mineral soil (n = 9). Sample collection was attempted during or shortly after each rainfall event from May–October; a partial vacuum (maximum 340 mbar) was applied such that water could be drawn into the lysimeter when soils were near field capacity. Successful sample collection proved to be irregular owing to the relatively dry nature of the soils. Following collection, soil water was stored at 4 °C until analysis. Soil water collected during 2007–2009 underwent analysis for SO_4^{2-}, NO_3^{-}, NH_4^{+}, Cl^{-}, Ca^{2+}, Mg^{2+}, Na^{+}, K^{+} and dissolved organic carbon, with total aluminum (Al) included as an analyte in 2008 and 2009.

Composite and bulk density (ρ) samples were collected from the forest floor (LFH: litter, fibric and humic) and rooting zone mineral horizons (Ae and Bj), of nine pits at the study site. Bulk density samples were collected from each mineral horizon using a volumetric sampling ring and hammer corer. Stone content was visually estimated, and depths of the rooting zone and individual horizons were measured after pit excavation. All composite and ρ samples were air-dried prior to analysis. Bulk density samples were sieved to 2 mm and weighed to determine ρ. Likewise, the composite samples were sieved such that all analyses were specific to the soil fraction (<2 mm) of the collected mineral substrate.

Mineral horizons were analyzed to determine organic matter content, pH, exchangeable base cation saturation, cation exchange capacity (CEC) and oxide content. Organic matter content was determined by measurement of loss-on-ignition after heating oven-dried soils at 400 °C for 12 hours in a muffle furnace. Soil pH was measured in deionized water after a 60 minute equilibration period (e.g. Lozano, 1987), using a 1:4 mass ratio. A two-step unbuffered salt extraction was used in the determination of exchangeable base cations and CEC (Lozano, 1987). Exchangeable base cations were removed from soil exchange sites with 1.0 M ammonium chloride (Cl^{-}) and analyzed by flame atomic absorption spectrophotometry (Varian™ 240FS). Sodium chloride was subsequently used to displace the NH_4^{+}, with concentrations in the extracts measured by colourimetry (SEAL™ AutoAnalyser 3 Quattro) and used to quantify CEC. Major oxide content of the soils was determined by fusion x-ray fluorescence.

A steady-state kinetic soil chemical model (PROFILE: Warfvinge and Sverdrup, 1992) was used to calculate mineral weathering rates from independent geophysical data. PROFILE is sensitive to mineralogy, soil surface area and moisture content (Hodson et al., 1996); ranges for each of these model inputs were used as a means of bounding base cation weathering rate estimates for the site. Mineralogy for soils at the site was calculated from oxide content using the computer program A2M (Posch and Kurz, 2007) based on known brunisol mineralogy in the region (Whitfield et al., 2010a). Minimum and maximum specific surface area for Ae and Bj horizons was characterized according to measurements for analogous sandy, quartz dominated soils in the AOSR (Whitfield and Reid, 2013). Soil moisture from surveys of sandy upland forest soils across the wider region (Whitfield and Watmough, 2012) was used to approximate the potential range in moisture content in PROFILE. Weathering rates were calculated separately for the Ae and Bj horizons.

2.4.4. Base cation and acid deposition

Ion exchange resin (IER) columns, essentially funnels attached to tubes containing ion exchange resin beads (Fenn and Poth, 2004; Simkin et al., 2004; Fenn et al., 2013; Fenn and Ross, 2010) were deployed under the forest canopy (n = 8) and in a nearby open clearing (n = 3–5), to measure throughfall and bulk deposition, respectively. Sulfur (as SO_4^{2-}) and nitrogen (as NO_3^{-} and NH_4^{+}) were measured during 2008–2011, while Ca^{2+}, Mg^{2+} and Na^{+} depositions were observed over a single year period (fall 2009 through fall 2010). The columns were deployed during two periods each year, with IER exposure typically lasting 5–7 months. Upon return to the lab, a KI elution was used to separate anions and cations from the resin and estimate areal deposition fluxes (Table 2). Nitrate and SO_4^{2-} were analyzed by ion chromatography and NH_4^{+} by colorimetry. For base cation analysis the IER columns were further extracted with KCl, and both the KI and KCl extracts were analyzed for base cations by ICP-AES (inductively coupled plasma atomic emission spectroscopy; Fenn et al., 2013).

In addition, Ca^{2+}, Mg^{2+} and Cl^{-} depositions were measured in throughfall at a more remote jack pine stand. These data were

Table 1
Selected average (standard deviation) physical and chemical properties of the mineral soil at the study site (n = 9 per horizon).

Soil parameters	LFH horizon	Ae horizon	Bj horizon
Sand (%)	-	83.8 (7.2)	87.6 (0.9)
Silt (%)	-	14.4 (6.7)	10.2 (0.7)
Clay (%)	-	1.8 (0.6)	2.2 (0.2)
BD (g cm^{-3})	-	0.85 (0.21)	1.56 (0.08)
Depth (cm)	2.6 (0.7)	5.1 (1.0)	34.9 (1.0)
pH	5.6 (1.3)	5.3 (0.2)	5.0 (0.1)
C/N	43.0 (7.9)	38.4 (6.2)	30.0 (2.3)
N (%)	0.82 (0.19)	0.06 (0.02)	0.01 (0.01)
S (%)	0.34 (0.05)	0.03 (0.01)	0.01 (0.01)
LOI (%)	70.5 (12.1)	6.0 (3.0)	1.0 (1.0)
ex-Ca ($mmol_c$ kg^{-1})	269 (103)	13.2 (9.6)	4.6 (1.7)
ex-Mg ($mmol_c$ kg^{-1})	67.2 (31.8)	2.2 (1.4)	1.3 (0.5)
ex-K ($mmol_c$ kg^{-1})	11.0 (5.1)	0.28 (0.10)	0.30 (0.07)
ex-Na ($mmol_c$ kg^{-1})	8.3 (2.7)	0.26 (0.09)	0.26 (0.06)
ex-Al ($mmol_c$ kg^{-1})	0.02 (0.010)	1.5 (0.9)	0.8 (90.2)
ex-Mn ($mmol_c$ kg^{-1})	1.49 (0.05)	1.1 (1.0)	0.36 (0.23)
ex-Fe ($mmol_c$ kg^{-1})	0.003 (0.005)	0.15 (0.04)	0.21 (0.02)
CEC ($mmol_c$ kg^{-1})	570 (120)	32.4 (19.3)	16.6 (4.8)
BS (%)	63.5 (21.0)	45.0 (20.2)	37.9 (3.0)

Table 2
Minimum and maximum estimates of annual total deposition to the study site, and the deposition flux after model calibration. For base cations a single best-estimate of annual flux is shown (as maximum).

Parameter	Units	Observation years	Min	Max	Calibrated
Ca^{2+}	$mmol_c$ m^{-2} yr^{-1}	1		160	160
Mg^{2+}	$mmol_c$ m^{-2} yr^{-1}	1		74	66
Na^{+}	$mmol_c$ m^{-2} yr^{-1}	1		47	38
K^{+}	$mmol_c$ m^{-2} yr^{-1}	1		10	10
S	$mmol_c$ m^{-2} yr^{-1}	3	113	203	118
NH_4^{+}	$mmol_c$ m^{-2} yr^{-1}	3	48	137	93
NO_3^{-}	$mmol_c$ m^{-2} yr^{-1}	3	39	58	49

used to estimate canopy leaching (12.5 and 1.7 $mmol_c\ m^{-2}\ yr^{-1}$, respectively for Ca^{2+} and Mg^{2+}) in order to approximate total deposition (from throughfall fluxes) of Ca^{2+} and Mg^{2+} at the study site. Given the limited capacity for canopy leaching of Cl^- and low spatial variability in deposition between the remote site and the study site indicated by a regional Cl deposition map (Vet and Shaw, 2004), total deposition at the study site was assumed equal to throughfall flux at the remote site. No measurement of K^+ deposition to the study site was available; instead an estimate from a regional deposition map (Vet and Shaw, 2004) was adjusted according to the observed (IER) Na enrichment factor (throughfall deposition: bulk deposition).

2.4.5. Deposition and forest growth scenarios

Historical deposition of S and N was constructed from a regional emissions inventory (e.g. Whitfield et al., 2009), with the model hindcast period spanning pre-development (1900) through the calibration year (2010). For simplicity, NH_3 and NO_x emissions were not distinguished from each other as they are poorly characterized in the region. While emission inventories for base cations are also not available, the location of the study site, being embedded among large scale industrial activities, suggests the development level will influence deposition of these elements. As such the historical base cation deposition sequences used in the current study reflect production levels, consistent with the behavior of N, with relatively small increases through the 1970s followed by rapid increases over the last two decades. Background (pre-development) deposition of base cations was estimated from a station (High Prairie) lying southwest of the AOSR but also in the Boreal Plains ecozone. This location should provide a reasonable estimate of historic base cation deposition as it is situated in an area of land cover character similar to the AOSR, but is by comparison relatively free of land clearing disturbances. A remote station in Snare Rapids, NWT considered to receive relatively pristine levels of atmospheric deposition was used to estimate background S and N deposition levels.

Future levels of atmospheric deposition at the study site remain unknown; however two future scenarios were used to demonstrate the influence of base cation deposition on soil chemistry (Fig. 2). A 'Constant' scenario assumes no change in deposition (from 2010 values) during the 50 year model forecast period (2011–2060). The second scenario ('Background') assumes no change in S or N deposition going forward, but an abrupt return to background deposition levels of Ca^{2+}, Mg^{2+}, Na^+, and K^+ for the duration of the forecast.

Sinks of Ca^{2+}, Mg^{2+} and K^+ associated with forest growth were included in the model, as were sources of these nutrients attributed to fire. Nutrient uptake was estimated according to above-ground pools for jack pine growing on sandy soils (Perala and Alban, 1982) normalizing for above-ground biomass. Uptake by the forest was assumed to occur over a 50-year period, approximating the fire return interval for the region. Likewise, Ca^{2+}, Mg^{2+} and K^+ held within the biomass were assumed to pulse back to the soil over a 10-year period following a fire event with the initial pulse of nutrients coinciding with the beginning of the uptake sequence and representing forest regeneration. This 50-year forest growth and fire cycle was parameterized in MAGIC to occur repeatedly over the period of model simulation.

2.4.6. Calibration procedure

The model was parameterized using inputs describing an aggregated uniform soil compartment consisting of the uppermost 0.25 m of mineral soil and overlying organic horizons (Table 3). Physicochemical properties for the LFH, Ae and Bj horizons were weighted according to depth and bulk density (ρ). An annual time step was used and the model was interactively calibrated to match observed and simulated variables in the year 2010. The target variables that were the focus of calibration included soil chemistry variables (exchangeable base cations and pH) and soil solution chemistry (base cation, SO_4^{2-}, NH_4^+, NO_3^-, Cl^- and Al concentrations). The maximum and minimum observations of annual average soil water concentrations (approximately 20 samples yr^{-1}) were used to bind the upper and lower limits for a successful calibration. Briefly, a number of parameters were subject to change as part of the calibration process (Table 3). Observed Cl^- concentration was used to refine the amount of soil water percolating through the soil layer such that a best approximation of natural hydrologic conditions was used. Nitrification and NO_3^- uptake processes were adjusted in order that simulated NH_4^+ and NO_3^- concentrations were within acceptable limits. Sulfur retention in the soils was specified through the SO_4^{2-} adsorption parameters; it was also necessary to calibrate S deposition amount (within the range of observations) in order to generate a simulation consistent with observed soil water SO_4^{2-} concentration. Base cation and total Al concentrations in soil solution and exchangeable base cations on the soil exchange sites were calibrated through iterative adjustment of the Al solubility and cation exchange coefficients as well as base cation weathering rates. It is acknowledged that close to the mines Al deposition has likely increased (Landis et al., 2012) but we have assumed that Al geochemistry is controlled primarily by the

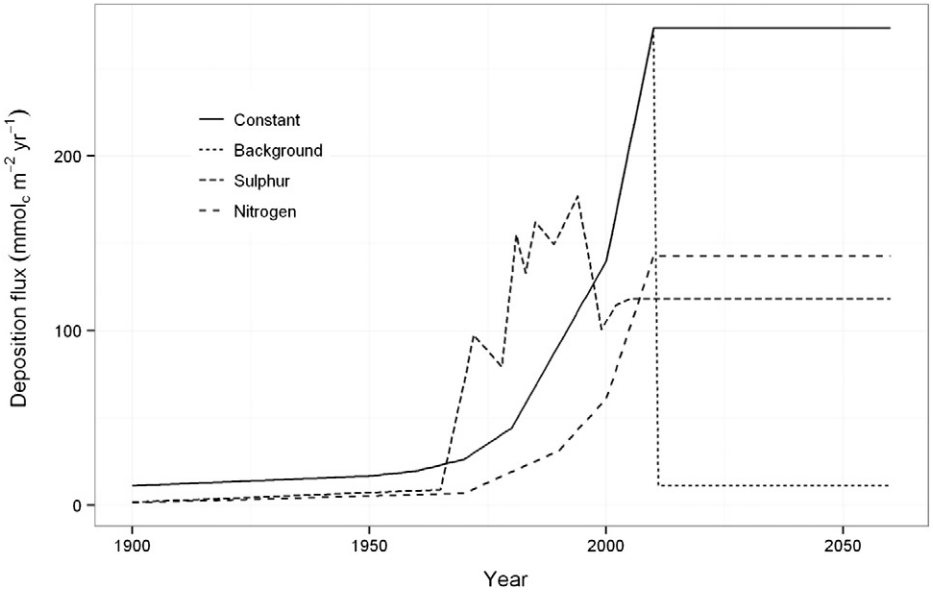

Fig. 2. Sulfur, nitrogen and base cation (Constant, Background) deposition scenarios at the intensive study site (see text for details).

Table 3
Calibrated soil parameters at the study site. Where site data were available, minimum, maximum or best estimate only (shown as maximum) parameter estimates are shown.

Parameter	Unit	Calibrated value	Min	Max
Dissolved organic carbon	$\mu mol\ L^{-1}$	225		
Aluminum solubility coefficient	log	10.75		
SO_4^{2-} adsorption half saturation	$\mu mol_c\ L^{-1}$	120		
SO_4^{2-} adsorption maximum capacity	$mmol_c\ kg^{-1}$	20.0		
Percolating water	m	0.104	0.094	0.158
Ca^{2+} weathering	$mmol_c\ m^{-2}\ yr^{-1}$	3.70	0.17	3.70
Mg^{2+} weathering	$mmol_c\ m^{-2}\ yr^{-1}$	0.10	0.10	2.00
Na^{+} weathering	$mmol_c\ m^{-2}\ yr^{-1}$	0.20	0.20	5.00
K^{+} weathering	$mmol_c\ m^{-2}\ yr^{-1}$	1.80	0.09	2.00
Ca^{2+} sink	$mmol_c\ m^{-2}\ yr^{-1}$	7.90		10.5
Mg^{2+} sink	$mmol_c\ m^{-2}\ yr^{-1}$	2.60		3.40
K^{+} sink	$mmol_c\ m^{-2}\ yr^{-1}$	2.40		3.10
Nitrification	%	99.4		
NO_3^{-} sink	%	99.8		
Ca^{2+} source	$mmol_c\ m^{-2}\ yr^{-1}$	7.90		
Mg^{2+} source	$mmol_c\ m^{-2}\ yr^{-1}$	2.60		
K^{+} source	$mmol_c\ m^{-2}\ yr^{-1}$	2.40		
Selectivity coefficient (Al-Ca)		-1.00		
Selectivity coefficient (Al-Mg)		0.25		
Selectivity coefficient (Al-Na)		-0.50		
Selectivity coefficient (Al-K)		-2.50		

large soil Al pool rather than by atmospherically deposited Al. In the case of Na^{+} and Mg^{2+}, simulated soil water concentrations exceeded the maximum observed values when the minimum weathering rates were used, thus small reductions to atmospheric deposition were necessary for model calibration of these elements (Table 4).

3. Results

3.1. Regional base cation weathering rates

Base cation (BC:Ca^{2+}, Mg^{2+}, K^{+} and Na^{+}) weathering rates at the 63 sites were very low, ranging from 1.6 to 73.9 $mmol_c\ m^{-2}\ yr^{-1}$, with a median base cation weathering rate of 17.0 $mmol_c\ m^{-2}\ yr^{-1}$ (Fig. 3). More than 80% (52 of 63) of the sites had a base cation weathering rate <40 $mmol_c\ m^{-2}\ yr^{-1}$ (Fig. 3).

Table 4
Lower (min) and upper (max) target window bounds for soil solution and soil chemistry, and simulated values for the calibration year (2010).

Parameter	Units	Min	Max	Simulated value
NH_4^{+}	$\mu mol_c\ L^{-1}$	1.80	6.30	4.70
NO_3^{-}	$\mu mol_c\ L^{-1}$	1.70	2.20	1.90
SO_4^{2-}	$\mu mol_c\ L^{-1}$	235	347	318
Cl^{-}	$\mu mol_c\ L^{-1}$	56.9	69.9	62.4
Total Al	$\mu mol_c\ L^{-1}$	48.3	98.3	51.9
Ca^{2+}	$\mu mol_c\ L^{-1}$	198	401	211
Mg^{2+}	$\mu mol_c\ L^{-1}$	95.9	159	143
Na^{+}	$\mu mol_c\ L^{-1}$	78.9	312	269
K^{+}	$\mu mol_c\ L^{-1}$	38.0	52.4	49.4
Base saturation	%	36.0	49.2	42.3
Exchangeable Ca	%	26.3	36.8	31.4
Exchangeable Mg	%	6.80	9.00	8.20
Exchangeable Na	%	1.30	1.60	1.50
Exchangeable K	%	1.60	1.80	1.30
pH soil		4.91	5.14	5.27

3.2. Regional atmospheric deposition

Atmospheric deposition of S, DIN (NO_3^{-} and NH_4^{+}) and base cations (Ca^{2+}, Mg^{2+} and Na^{+}) in throughfall was approximately double the amount recorded in open collectors and decreased logarithmically with distance from the center of the industrial activities center (Fig. 4). Within about 20 km of the industrial center annual acid (S + N) deposition could be as high as 180 $mmol_c\ m^{-2}\ yr^{-1}$ in open collectors and up to 360 $mmol_c\ m^{-2}\ yr^{-1}$ in throughfall. Beyond 75 km, acid deposition was <30 $mmol_c\ m^{-2}\ yr^{-1}$in both open collectors and throughfall (Fig. 4). In mass units throughfall deposition of DIN from 2008 to 2011 within 20 km of the industrial center ranged from 3–25 kg N $ha^{-1}\ yr^{-1}$ compared to 8–38 kg $ha^{-1}\ yr^{-1}$ for S. At sites greater than 75 km from the industrial center throughfall deposition of DIN generally ranged from 1–2 kg N $ha^{-1}\ yr^{-1}$ compared to S deposition of 2–4 kg $ha^{-1}\ yr^{-1}$. Deposition of S typically exceeded DIN deposition in the winter: the average S:DIN ratio in open collectors in the winter was 2.0 and varied between 0.8 and 4.6, while in summer the average S:DIN ratio was 1.1, ranging from 0.5 to 2.1. Base cation deposition was dominated by Ca^{2+}, which comprised approximately 71% of the total base cations (Ca^{2+}, Mg^{2+} and Na^{+}) measured in open collectors and 63% of base cations in throughfall. Calcium and Mg^{2+} were strongly correlated in both throughfall ($r^2 = 0.82$; $p < 0.001$) and in open collectors ($r^2 = 0.78$; $p < 0.001$), with an average Ca:Mg ratio (mol_c/mol_c) of 2.4 ± 1.1 (S.D.) in throughfall and 4.0 ± 1.5 in open collectors (Fig. 5). Base cation deposition (Ca^{2+}, Mg^{2+} and Na^{+}) in throughfall and in open collectors was comparable to S + N deposition, particularly close to the industrial center where annual base cation deposition could be as high as 202 $mmol_c\ m^{-2}\ yr^{-1}$in open collectors and up to 336 $mmol_c\ m^{-2}\ yr^{-1}$in throughfall (Fig. 4). The Ca + Mg:S ratio (mol_c/mol_c) in throughfall and open collectors was variable but typically >1.0, especially in the summer months (Fig. 6).

3.3. Dynamic modeling at the intensive study site

Sulfur and DIN deposition measured in throughfall during the three years was between 113–203 and 87–195 $mmol_c\ m^{-2}\ yr^{-1}$, respectively (Table 2). Base cation (Ca^{2+}, Mg^{2+} and Na^{+}) deposition measured in throughfall during a single year was 311 $mmol_c\ m^{-2}\ yr^{-1}$, with an average Ca:Mg ratio ($mol_c\ mol_c^{-1}$) of 2.4, and base cation deposition was greater than S + DIN deposition (Table 2). The dominant minerals that contribute to base cation weathering at the site were K-feldspar,

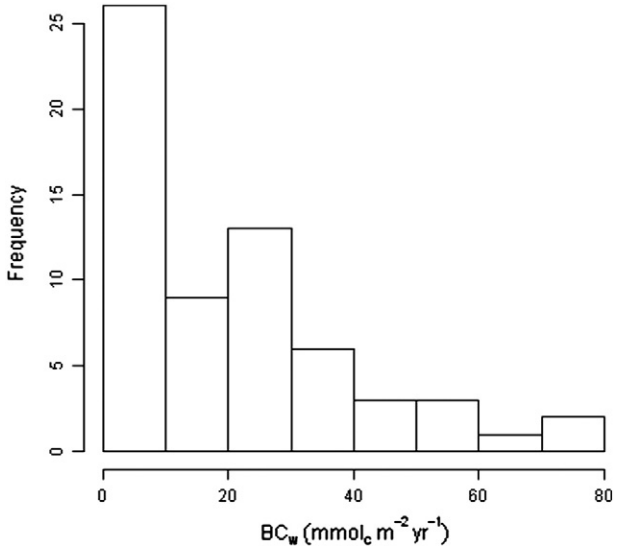

Fig. 3. Estimates of rooting zone (0.5 m) base cation weathering rates (BC_w) for all soil plots in the AOSR where PROFILE has been applied (n = 63). Minimum and maximum estimates of BC_w for soils of the forest stand considered in the current study are included.

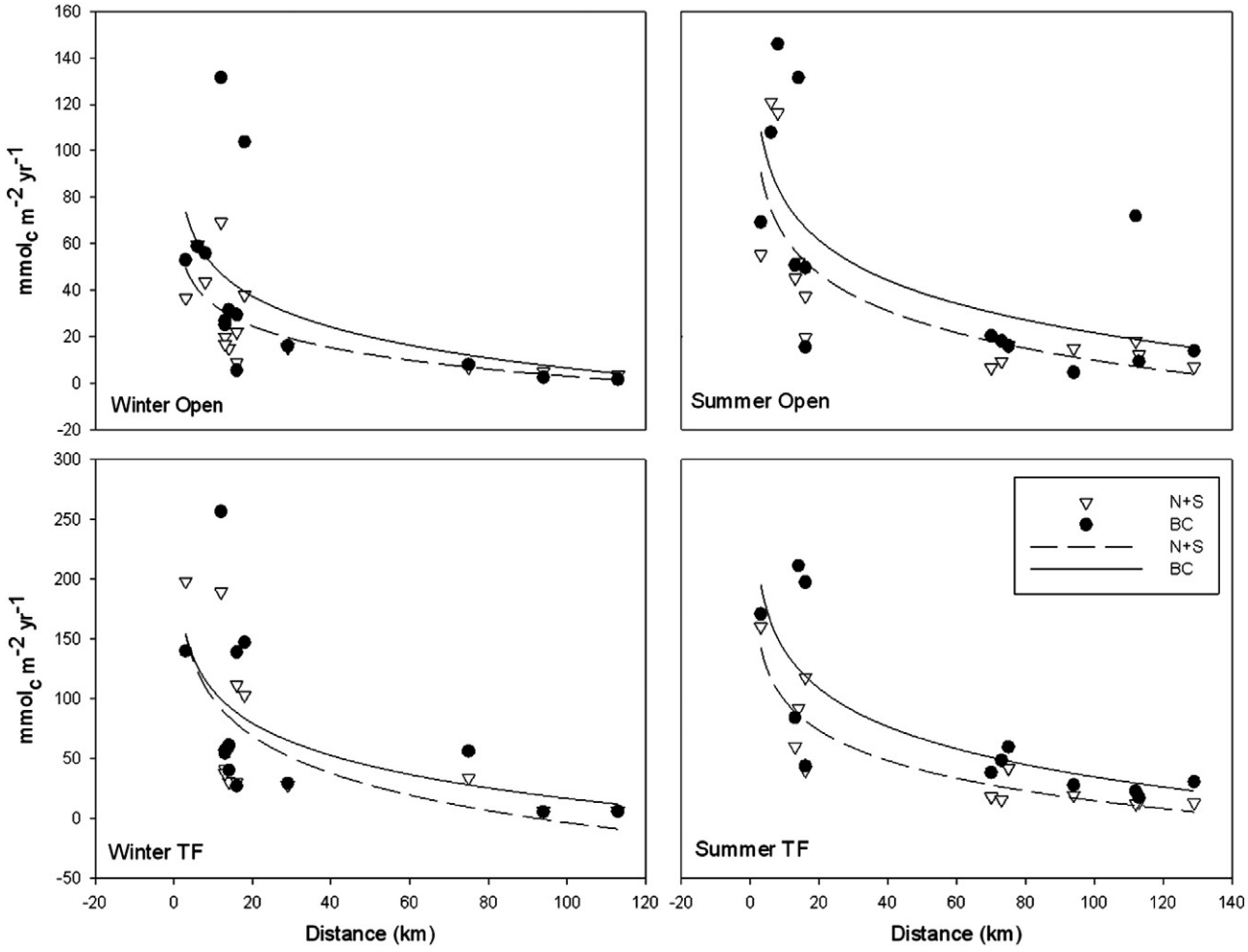

Fig. 4. Comparison of base cation deposition ($Na^{2+} + Mg^{2+} + Ca^{2+}$) and DIN + SO_4^{2-} deposition in forest clearings (bulk deposition in open areas) and in throughfall versus distance from the industrial center. The N + S and base cation data are from October 2009 to May 2010 (winter) and May 2010 to October 2010 (summer).

vermiculite, dolomite and actinolite, but calibrated base cation weathering rates were low (5.8 $mmol_c\ m^{-2}\ yr^{-1}$) (Table 5). The calibrated Ca^{2+} weathering rate at the intensive study site was 3.7 $mmol_c\ m^{-2}\ yr^{-1}$, which was much higher than the calibrated Mg weathering rate of 0.1 $mmol_c\ m^{-2}\ yr^{-1}$ (Table 3). Despite the high level of acid deposition and low base cation weathering rate, the average Ca^{2+} and Mg^{2+} concentrations in soil solution were 289 ± 119 (S.D.) and 132 ± 53 $\mu mol_c\ L^{-1}$, respectively (based on measurement of approximately 20 samples yr^{-1}). Calcium and Mg^{2+} concentrations measured in individual lysimeter samples were very strongly correlated with an average Ca:Mg ratio ($mol_c\ mol_c^{-1}$) of 2.2 ± 0.4, which is similar to that in throughfall at the site (Fig. 7).

Model calibrations to soil solution and soil exchangeable base cation fractions yielded good agreement between simulated and observed (target) values (Table 4). The target windows for several of the parameters were quite wide owing to large observed variability in soil solution chemistry (e.g. Na^+). Nevertheless, the simulated values resulting from the calibration procedure were generally closer to the center of the target window than the bounds. The simulated result for pH during the calibration year was one exception, as it did not fall within the range of observations, however there is uncertainty associated with the targets used for pH as they were defined according to laboratory estimates (see methods) rather than *in-situ* measurement. Accordingly, given the small difference between simulated pH and the upper limit for the pH target window (0.1 units, comparable to common level of accuracy for pH probes), the model simulation of soil solution pH appears to be reasonable.

Model simulations of soil and soil solution chemistry reflect the changes in atmospheric deposition during the last century, with changes in BS, and pH being most pronounced during the last decade coinciding with the period of peak deposition fluxes (Fig. 8). Base saturation increased steadily during the 20th century from a background level of approximately 10% to the current level of 42%. Short-term (and transient) periods of rapid increase result post-fire due to a pulse of base cations to the soil compartment. Similarly, historical pH responded primarily to the forest-fire events that were parameterized as part of the model application, with rapid (albeit small) increases in the years immediately following fire events, followed by gradual decline toward the pre-fire level. This is consistent with the return of base cations to the soil (and increased BS) from the vegetation. There was a negligible increase in simulated Ca:Al ratio during the model hindcast.

MAGIC simulations of future soil and soil solution chemistry under two different base cation deposition scenarios revealed contrasting results. In contrast to the stable Ca:Al during the 20th and early 21st century, the model simulations suggest this metric is presently responding to elevated base cation deposition. Under conditions of constant (at current levels) base cation and acid deposition, large increases in Ca:Al are predicted. Similarly, future increases in BS are simulated during the next ~25 years, at which point cation exchange sites on the soil are anticipated to effectively be filled by base cations (Fig. 8). Substantial increases in pH are also forecast for persisting conditions of high base cation deposition. Under the second (Background) scenario, where base cation deposition undergoes a step change to

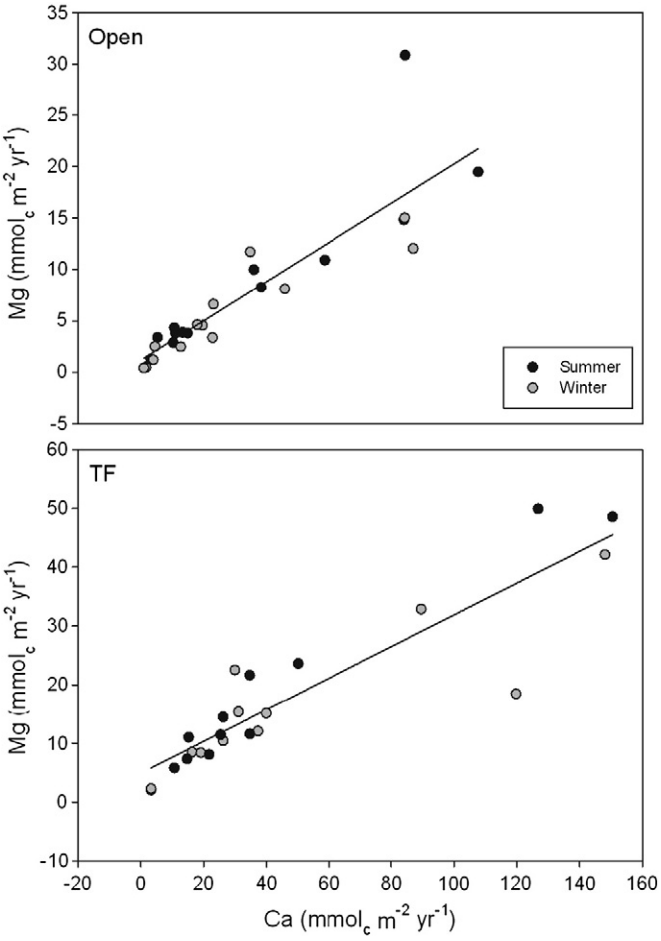

Fig. 5. Relationship between Ca and Mg deposition at open and throughfall (TF) sites collected using ion exchange columns placed in situ during the summer and winter 2009–2010.

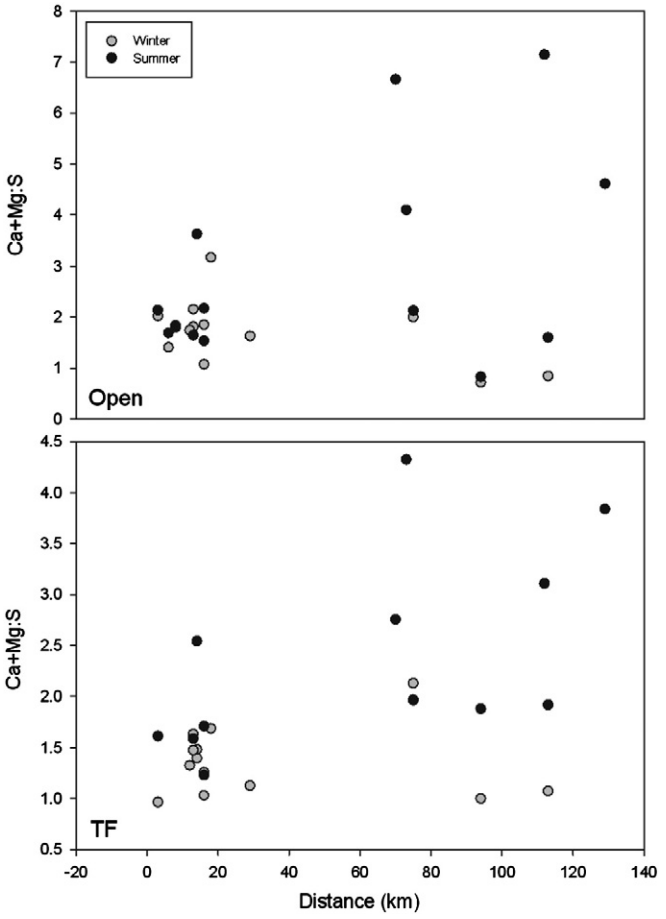

Fig. 6. Ca + Mg:S ratios in bulk deposition (open areas) and in throughfall (TF) versus distance from the industrial center.

background levels (S and N remain constant) at the outset of the forecast simulation, BS returns to background levels within the timeframe of the 50 year forecast. In contrast, pH is simulated to decrease to a level lower than the modeled background condition; depression of pH below background (0.2 pH units) in this scenario is the result of elevated S deposition, as N leaching, as parameterized, will remain low in this scenario. Likewise under conditions of low future base cation deposition, slight decreases in Ca:Al were simulated (0.57 in 2060 versus background of 0.87). At the outset of the forecast period, there is a slight delay prior to the simulated decreases in BS and pH (Fig. 8) despite the large decrease in base cation deposition due to a pulse of base cations to the soil compartment consistent with the forest fire/growth sequence parameterized in the model.

4. Discussion

Base cation weathering rates at the 63 acid-sensitive sites, which were distributed widely across the region, were among some of the lowest values reported in the literature (e.g. Ouimet, 2008; Koseva et al., 2010; Whitfield et al., 2011). The median base cation weathering rate was just 17 mmol$_c$ m^{-2} yr^{-1} and more than 80% (52 of 63) of the sites had a base cation weathering rate <40 mmol$_c$ m^{-2} yr^{-1}. These weathering estimates are at the lower end of weathering estimates for soils in other parts of Canada: base cation weathering rates for the soil rooting zone of 3–13 mmol$_c$ m^{-2} yr^{-1} (Nova Scotia: Whitfield et al., 2006); 58–446 mmol$_c$ m^{-2} yr^{-1} (Quebec: Houle et al., 2012); 21 –79 mmol$_c$ m^{-2} yr^{-1} (Ontario: Koseva et al., 2010); 0.1–8000 mmol$_c$ m^{-2} yr^{-1} (Saskatchewan: Whitfield and Watmough, 2012); and 19–351 mmol$_c$ m^{-2} yr^{-1} (British Columbia: Mongeon et al., 2010). Weathering rates in this study were estimated using PROFILE, which like all methods used to estimate base cation weathering rates, is associated with some uncertainties (Hodson and Langan, 1999). In a recent study Klaminder et al. (2011) compared weathering rates at a catchment in Sweden obtained using nine different methods and argued that uncertainty associated with weathering rates hampers policy decisions (in this case forestry) that need reliable base cation weathering rate estimates. Other studies however have found generally reasonable agreement among the various methods used to estimate base cation weathering rates (Starr et al., 1998; Whitfield et al., 2006). Previous work in the study region (AOSR) used the Zr-depletion method and the Pedological Mass Balance method to estimate base cation weathering rates for 33 soil profiles and reported weathering estimates ranges of 0–51 mmol$_c$ m^{-2} yr^{-1} and 0–58 mmol$_c$ m^{-2} yr^{-1}, respectively (Whitfield et al., 2011), which is within the range of values reported in this study. Similarly, the Soil Texture Approximation method was applied to 290 sites in the region and values of between 0 and 74 mmol$_c$ m^{-2} yr^{-1} were reported, with a median value of 10 mmol$_c$ m^{-2} yr^{-1} (Whitfield et al., 2010a). Overall, this study and previous work indicate that weathering rates of the acid-sensitive soils in the region are generally very low and are thus highly sensitive to increased acid deposition levels.

Close (<20 km) to the industrial center, acid (S + N) deposition in throughfall and open collectors was very high, approaching 360 mmol$_c$ m^{-2} yr^{-1} in throughfall and 180 mmol$_c$ m^{-2} yr^{-1} in open collectors. Acid deposition declined logarithmically with distance from the industrial center, such that S + N deposition was <30 mmol$_c$ m^{-2} yr^{-1} beyond 75 km from the industrial center. Acid deposition measured in throughfall was approximately double the amount

Table 5
Soil properties used as input for PROFILE, including minimum and maximum estimates used to bound the weathering rate, where appropriate.

Parameter	Units	A horizon		B horizon	
		Min	Max	Min	Max
Temperature	°C	3.5	4.0	3.4	3.9
Soil layer height	m	0.041	0.061	0.339	0.359
Water content	$m^3\ m^{-3}$	0.01	0.15	0.03	0.17
Dry soil bulk density	$kg\ m^{-3}$	640	1060	1480	1640
Surface area	$m^2\ m^{-3}$	44800	84800	2427200	3804800
Dissolved organic carbon	$mg\ L^{-1}$	15	15	15	15
CO_2 partial pressure[a]	x atm	10	10	10	10
log Kgibb[a]		8.5	8.5	8.5	8.5
Aluminum exponent[a]		3	3	3	3
K-Feldspar	%	1.53	2.56	1.53	2.56
Kaolinite	%	0.20	0.33	0.20	0.33
Plagioclase	%	0.10	0.16	0.10	0.16
Albite	%	0.55	0.92	0.55	0.92
Anorthite	%	0.03	0.05	0.03	0.05
Vermiculite	%	1.42	2.36	1.42	2.36
Muscovite	%	0.70	1.16	0.70	1.16
Illite	%	0.33	0.55	0.33	0.55
Apatite	%	0.03	0.05	0.03	0.05
Actinolite	%	1.48	2.47	1.48	2.47
Fe-Chlorite	%	0.04	0.06	0.04	0.06
Dolomite	%	0.03	0.04	0.03	0.04
Calcite	%	0.006	0.010	0.006	0.010
Hornblende	%	0	0	0	0

[a] Default parameter. All other parameters based on site information.

measured in open collectors, likely due to enhanced dry deposition beneath the forest canopies (Lovett and Lindberg, 1993). The levels of acid deposition measured within 20 km of the industrial center are greater than values recorded in the 1970s and 80s in eastern North America (Schindler, 1988) and are similar to values reported in central Europe around the same period, where widespread acidification impacts were reported (Dise and Wright, 1995). They are also currently comparable to acid deposition levels in parts of China, where there are concerns over ecosystem acidification (Zhang, 2006; Guo et al., 2010). In addition, S was generally the dominant component of acid deposition although S:DIN ratios varied between around 0.5 and 4.6, depending on location, type of collectors (open versus throughfall) and season. The fact that S is a major contributor to acid deposition is important because forests in the region are N-limited (Laxton et al., 2010) and there is no evidence of NO_3^- leaching from the rooting zone and so N does not presently contribute to soil acidification (Laxton et al., 2012). In contrast, the relatively young soils in the region typically have a very low SO_4^{2-} adsorption capacity (Whitfield et al., 2010c). Whitfield et al. (2010c) reported that the SO_4^{2-} adsorption capacity of soils in two acid-sensitive catchments was low relative to the comparably glaciated acid-sensitive soils of the north-eastern United States (e.g.,

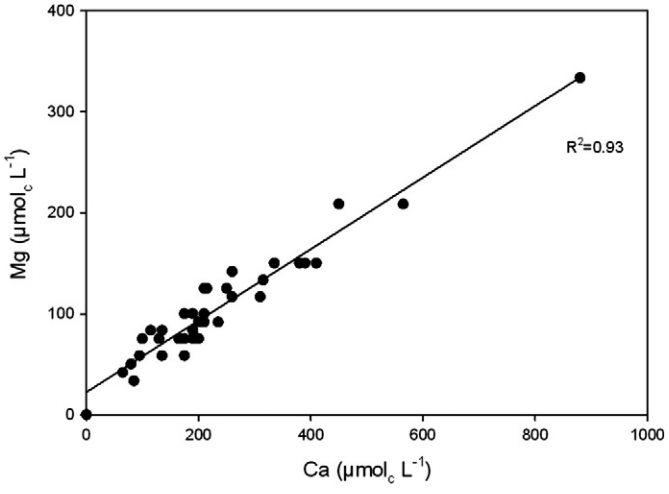

Fig. 7. Relationship between monthly Ca and Mg concentration in soil water collected at 0.25 m depth between 2007 and 2009 at the intensive study site.

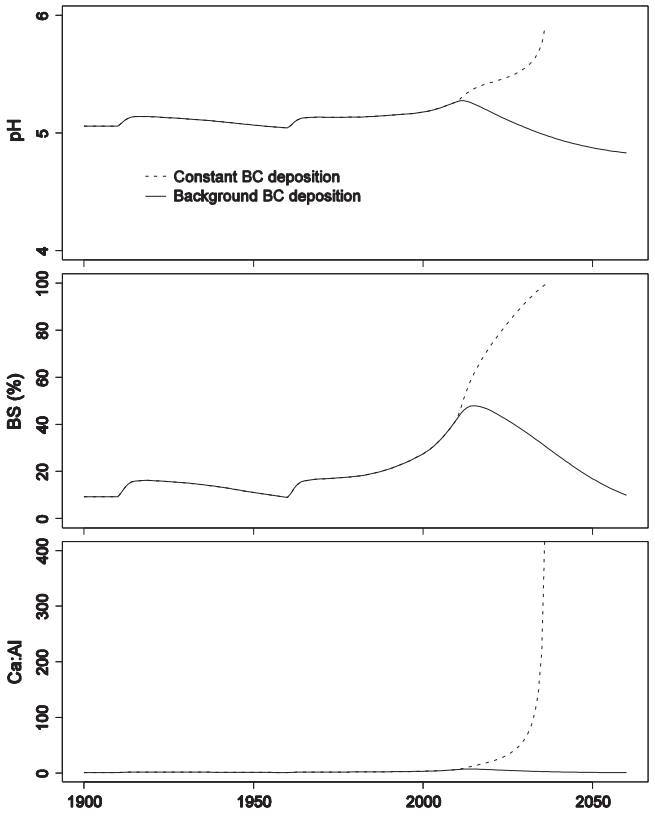

Fig. 8. Simulated changes in soil solution pH, soil base saturation, and soil solution molar Ca:Al ratio. Future scenarios assume constant (at current level) sulfur, nitrogen and base cation deposition (dashed line) and constant S and N deposition but background base cation deposition (solid line).

Nodvin et al., 1986) and to older soils in the south-eastern United States (e.g., Shanley, 1992). Consequently, very little S will be retained in the sandy, acid-sensitive soils and high levels of S deposition may be expected to cause soil acidification (Whitfield et al., 2010a).

The potential risk of soil acidification in the region however appears to be mitigated by the high levels of base cation deposition. Base cation deposition follows a similar pattern to acid deposition; being typically twice as high in throughfall compared with open collectors and declining logarithmically with distance from the industrial center. For most of the collection periods at most sites, base cation (Ca^{2+}, Mg^{2+} and Na^{+}) deposition exceeded acid (S, DIN) deposition in both throughfall and in open collectors. Larssen and Carmichael (2000) demonstrated how important base cation deposition was for neutralizing acid deposition in China, and Hedin et al. (1994) attributed the limited chemical recovery in surface waters from reductions in acid deposition to declining base cation deposition. Larssen and Carmichael (2000) suggested that a Ca:S ratio in wet deposition could be used to assess the risk associated with elevated acid deposition with values <1.0 signifying a potential risk.

In the present study, Ca^{2+} and Mg^{2+} in open collectors and throughfall are strongly correlated, suggesting a common source and thus we have used the Ca + Mg:S ratio to evaluate the potential risk of soil acidification. In almost all cases, the Ca + Mg:S ratio was greater than unity and tended to be much higher in summer than in winter indicating minimal risk of soil acidification as long as N is retained. The fact that the Ca + Mg:S ratio is generally higher in summer compared with winter supports the argument that base cations, S and N deposition are mostly derived from different sources (Landis et al., 2012). While most of the S is emitted from the up-grader stacks (Landis et al., 2012), N emissions are from several sources and surprisingly NH_4^+ deposition is often greater than NO_3^- deposition (Fenn and Ross, 2010; M.E. Fenn unpublished data). In contrast, base cation emissions appear to be derived primarily from dust associated with mining activities (Landis et al., 2012). Haul roads are constructed with mined materials (limestone overburden and low grade oil sand) and is a fugitive dust source due to mining-related traffic on these roads (Landis et al., 2012). Based on two grab samples from different haul roads, Ca^{2+} values of 28 + 24 g kg^{-1} and Mg^{2+} values of 6.3 + 3.1 g kg^{-1} were reported (Landis et al., 2012), representing an average Ca:Mg (mol_c/mol_c) ratio of 2.6. The average Ca:Mg ratio in throughfall was 2.4 ± 1.1 and the average Ca:Mg ratio in open collectors was 4.0 ± 1.5, which are not too dissimilar to the ratio in dust. The lower Ca:Mg ratio in throughfall relative to bulk deposition may be due to relatively greater canopy leaching of Mg compared with Ca (De Schrijver et al., 2004). The lower Ca + Mg:S ratios measured in winter may reflect the fact that the haul roads are likely covered with snow and ice and hence dust emissions will be reduced.

In the AOSR the regional effects-based emissions management framework stipulates that no further emission increases will be permitted if model simulations indicate that BS or BC:Al thresholds will be reached within 30 years and emission reductions are required if model simulations predict that chemical thresholds will be reached within 15 years. Whitfield et al. (2009) reported that changes in soil solution BC:Al ratio will likely be more sensitive than changes in soil BS, but soil solution chemistry is not monitored regionally. We modeled the response of soil and soil solution chemistry to deposition at the one site where soil solution chemistry is available, assuming either constant deposition or a reduction in base cation deposition to background levels. Sulfur and DIN deposition measured in throughfall at the site during the three years was between 113–203 and 87–177 $mmol_c\ m^{-2}\ yr^{-1}$, respectively. Base cation (Ca^{2+}, Mg^{2+} and Na^{+}) deposition measured in throughfall during a single year was 311 $mmol_c\ m^{-2}\ yr^{-1}$, with an average Ca:Mg ratio of 2.4, and was greater than S + DIN deposition. Soil solution has been monitored for three years at this site and NO_3^- concentrations in soil water at 25 cm depth are <5 $\mu mol_c\ L^{-1}$ indicating that presently almost all of the N in deposition is currently retained in soil or in vegetation, whereas SO_4^{2-} concentrations in soil solution are >235 $\mu mol_c\ L^{-1}$. Despite the high level of acid deposition and low base cation weathering rate (~6 $mmol_c\ m^{-2}\ yr^{-1}$), the average Ca^{2+} and Mg^{2+} concentrations were high; 289 and 132 $\mu mol_c\ L^{-1}$ respectively. Calcium and Mg^{2+} concentrations measured in individual lysimeter samples were very strongly correlated with a Ca:Mg ratio of approximately 2.2, which is similar to that in throughfall demonstrating the strong influence of base cation deposition on soil solution chemistry at the study site.

Model simulations indicate that historically soil and soil solution chemistry was relatively consistent, with slight perturbations following forest fires. Assuming that current levels of acid and base cation deposition persist, however, soil base saturation and the soil solution Ca:Al ratio and pH will increase rapidly within a few decades. While this will increase the sub-surface exchangeable base cation pool by approximately an order of magnitude, the absolute size of the pool is nonetheless limited by low CEC of these sandy, quartz dominated soils. Increased rooting zone availability of base cations due to high atmospheric deposition may benefit the vegetation of these nutrient poor soils. In the future event that Ca + Mg:S is lowered to less than unity, or N leaching results in acid deposition exceeding base cation deposition, this added pool of base cations will prove beneficial as it will increase the response time before soils and soil solution return to pH, BS or Ca:Al at or below their historical levels. In this region, where forest soil weathering reactions yield very small amounts of base cations, the balance between acidic and base cation inputs from deposition is of critical importance. As illustrated under the Background scenario, if base cation deposition is reduced to pre-development levels (and S and N are unchanged from current levels) there will be a dramatic reduction in soil base saturation, pH and Ca:Al to levels that could be detrimental to tree health (Cronan and Grigal, 1995). Monitoring of base cation deposition, in addition to the current focus on S and N, would add considerably to the robustness of acidification assessments for this region where active industrialization exerts near-constant change. One final point is that while base cation deposition in dust appears to prevent soil acidification, high deposition levels of metals such as Fe or Al may have undesirable consequences that should be investigated.

5. Summary

Sandy, acid-sensitive upland forest soils in the AOSR are widespread and have some of the lowest weathering rates reported in Canada and are thus highly sensitive to acid deposition, which within 20 km of the industrial center is greatly elevated and is comparable to, or even greater than, the high levels reported in central Europe and eastern North America during the “heyday” of acid deposition. Acid deposition in throughfall is about twice as high as deposition measured in open collectors and declines logarithmically with distance from the industrial activities. Despite the high level of acid deposition and highly sensitive nature of the soils, the risk of soil acidification is minimal due to the high levels of base cation deposition. The Ca + Mg:S ratios in both throughfall and in open collectors are typically greater than 1.0, suggesting that as long as N continues to be retained in soils there is little risk of soil acidification and in fact soil base saturation and pH may be expected to increase. In contrast to S, emissions of base cations are poorly quantified as they are mostly derived form fugitive dust sources in the mines.

Acknowledgments

The authors would like to thank CEMA and WBEA for logistical support and the provision of data and financial support. Support for CJW was provided through an NSERC Post-Doctoral Fellowship.

References

Abboud SA, Turchenek LW, Halsey LA. Critical loads of acid deposition on soils in the Athabasca Oil Sands Region, Alberta. NO_x–SO_2 Management Working Group Cumulative Environmental Management Association; 2002.

Agriculture and Agri-Food Canada. The Canadian System of Soil Classification. 3rd ed. Ottawa, Canada: AAFC; 1998.

Cosby BJ, Hornberger GM, Galloway JN, Wright RF. Modeling the effects of acid deposition: assessment of a lumped parameter model of soil water and streamwater chemistry. Water Resour Res 1985;21:51–63.

Cosby BJ, Ferrier RC, Jenkins A, Wright RF. Modelling the effects of acid deposition: refinements, adjustments and inclusion of nitrogen dynamics in the MAGIC model. Hydrol Earth Syst Sci 2001;5(3):499–518.

Cronan CS, Grigal DF. Use of calcium/aluminum ratios as indicators of stress in forest ecosystems. J Environ Qual 1995;24(2):209–26.

Davies MJE. Air quality modeling in the Athabasca Oil Sands Region. Alberta Oil Sands: Energy, Industry and the Environment. Oxford, UK: Elsevier Press; 2012. p. 267–309.

De Schrijver A, Nachtergale L, Staelens J, Luyssaert S, De Keersmaeker L. Comparison of throughfall and soil solution chemistry between a high density Corsican pine stand a naturally regenerated silver birch stand. Environ Pollut 2004;131:93–105.

Dise NB, Wright RF. Nitrogen leaching from European forests in relation to nitrogen deposition. For Ecol Manag 1995;71:153–61.

Environment Canada. The state of Canada's environment directorate – 1996. Available at: www.ec.gc.ca/soer-ree/English/SOER/1996report/Doc/1-6-2-4-1.cfm, 1996.

Fenn ME, Poth MA. Monitoring nitrogen deposition in throughfall using ion exchange resin columns: a field test in the San Bernardino Mountains. J Environ Qual 2004; 33:2007–14.

Fenn ME, Ross CS. Sulfur and nitrogen deposition monitoring in the Athabasca Oil Sands Region. Extended Abstract 2010-A-664-AWMAProceedings of the Air and Waste Management Association 103rd Annual Conference and Exhibition, Calgary, Alberta, Canada, June 22-25, 2010; 2010.

Fenn ME, Ross CS, Schilling SL, Baccus WD, Larrabee MA, Lofgren RA. Atmospheric deposition of nitrogen and sulfur and preferential canopy consumption of nitrate in the forests of the Pacific Northwest, USA. For Ecol Manage 2013;302:240–53.

Guo JH, Liu XJ, Zhang Y, Shen JL, Han WX, Zhang WF, et al. Significant acidification in major Chinese croplands. Science 2010;327(5968):1008–10.

Hazewinkel RRO, Wolfe AP, Pla S, Curtis C, Hadley K. Have atmospheric emissions from the Athabasca Oil Sands acidified lakes in northeastern Alberta, Canada? Can J Fish Aquat Sci 2008;65:1554–67.

Hedin LO, Granat L, Likens GE, Buishand TA, Galloway JN, Butler TJ, et al. Steep declines in atmospheric base cations in regions of Europe and North America. Nature 1994;367: 351–4.

Hodson ME, Langan SJ, Wilson MJ. A sensitivity analysis of the PROFILE model in relation to the calculation of soil weathering rates. Appl Geochem 1996;11(6):835–44.

Hodson ME, Langan SJ. Considerations of uncertainty in setting critical loads of acidity of soils: the role of weathering rate determination. Environ Pollut 1999;106(1):73–81.

Holowaychuk N, Fessenden RJ. Soil sensitivity to acid deposition and the potential of soils and geology in Alberta to reduce the acidity of acidic inputs. Alberta Research Council, Earth Science Report 87-1, Edmonton, AB; 1987 (43 pp.).

Houle D, Lamoureux P, Bélanger N, Bouchard M, Gagnon C, Couture S, et al. Soil weathering rates in 21 catchments of the Canadian Shield. Hydrol Earth Syst Sci 2012;16(3):685–97. http://dx.doi.org/10.5194/hess-16-685-2012.

Jung K, Chang SX, Ok YS, Arshad MA. Critical loads and H^+ budgets of forest soils affected by air pollution from oil sands mining in Alberta, Canada. Atmos Environ 2013;69: 56–64.

Klaminder J, Lucas RW, Futter MN, Bishop KH, Köhler SJ, Egnell G, et al. Silicate mineral weathering rate estimates: are they precise enough to be useful when predicting the recovery of nutrient pools after harvesting? For Ecol Manag 2011;261(1):1–9.

Koseva IS, Watmough SA, Aherne J. Estimating base cation weathering rates in Canadian forest soils using a simple texture-based model. Biogeochemistry 2010;101(1–3): 183–96.

Landis MS, Pancras JP, Graney JR, Stevens RK, Percy KE, Krupa S. Receptor modeling of epiphytic lichens to elucidate the sources and spatial distribution of inorganic air pollution in the Athabasca Oil Sands Region. Alberta Oil Sands: Energy, Industry and the Environment. Oxford, UK: Elsevier Press; 2012. p. 427–67.

Larssen T, Carmichael GR. Acid rain and acidification in China: the importance of base cation deposition. Environ Pollut 2000;110(1):89–102.

Laxton DL, Watmough SA, Aherne J, Straker J. An assessment of nitrogen saturation in *Pinus banksiana* plots in the Athabasca Oil Sands Region, Alberta. J Limnol 2010; 69(1s):171–80.

Laxton DL, Watmough SA, Aherne J. Nitrogen cycling in *Pinus banksiana* and *Populus tremuloides* stands in the Athabasca oil sands region, Alberta, Canada. Water Air Soil Pollut 2012;223(1):1–13.

Lovett GM, Lindberg SE. Atmospheric deposition and canopy interactions of nitrogen in forests. Can J Forest Res 1993;23:1603–16.

Lozano F. Physical and chemical properties of the soils at the Southern Biogeochemistry study site. Dorset, Ontario: Dorset Research Centre, Ontario Ministry of Environment; 1987 (Report no. BGC-018).

Mongeon A, Aherne J, Watmough SA. Steady-state critical loads of acidity for forest soils in the Georgia Basin, British Columbia. J Limnol 2010;69(1s):193–200.

Nellemann C, Thomsen MG. Long-term changes in forest growth: potential effects of nitrogen deposition and acidification. Water Air Soil Pollut 2001;128(3–4):197–205.

Nodvin SC, Driscoll CT, Likens GE. The effect of pH on sulfate adsorption by a forest soil. Soil Sci 1986;142(2):69–75.

Ouimet R. Using compositional change within soil profiles for modelling base cation transport and chemical weathering. Geoderma 2008;145(3):410–8.

Perala DA, Alban DH. Biomass, nutrient distribution and litterfall in Populus, Pinus and Picea stands on two different soils in Minnesota. Plant Soil 1982;64(2):177–92.

Percy KE. Geoscience of Climate and Energy 11. Ambient air quality and linkage to ecosystem in the Athabasca Oil Sands, Alberta. Geosci Can 2013;40(3):182–201.

Posch M, Kurz D. A2M—a program to compute all possible mineral modes from geochemical analyses. Comput Geosci 2007;33(4):563–72.

Proemse BC, Mayer B, Fenn ME. Tracing industrial sulfur emissions in atmospheric sulfate deposition in the Athabasca oil sands region, Alberta, Canada. Appl Geochem 2012; 27:2425–34.

Schindler DW. Effects of acid rain on freshwater ecosystems. Science 1988;239(4836): 149–57.

Shanley JB. Sulfate retention and release in soils at Panola Mountain, Georgia. Soil Sci 1992;153(6):499–508.

Simkin SM, Lewis DN, Weathers KC, Lovett GM, Schwarz K. Determination of sulfate, nitrate, and chloride in throughfall using ion-exchange resins. Water Air Soil Pollut 2004;153:343–54.

Soil Classification Working Group. The Canadian system of soil classification Publ; 1998. p. 187 (1646, Revised).

Starr M, Lindroos AJ, Tarvainen T, Tanskanen H. Weathering rates in the Hietajärvi integrated monitoring catchment. Boreal Environ Res 1998;3:275–85.

Stringham G. Energy Developments in Canada's Oil Sands. Alberta Oil Sands: Energy, Industry and the. Environment 2012;11:19.

Turchenek LW, Abboud SA, Tomas CJ, Fessenden RJ, Holowaychuk N. Effects of acid deposition on Alberta soils. Calgary, Alberta: Alberta Research Council Terrain Sciences Department; 1987.

Vet R, Shaw M. 1994–1998 average dry deposition velocities calculated using the MSC Air Quality Research Branch dry deposition model (RDM). Toronto, Ontario: Meteorological Service of Canada, Environment Canada; 2004.

Warfvinge P, Sverdrup H. Calculating critical loads of acid deposition with PROFILE – a steady-state soil chemistry model. Water Air Soil Pollut 1992;63:119–43.

Whitfield CJ, Watmough SA, Aherne J, Dillon PJ. A comparison of weathering rates for acid sensitive catchments in Nova Scotia, Canada and their impact on critical load calculations. Geoderma 2006;136(3):899–911.

Whitfield CJ, Aherne J, Watmough SA. Modeling soil acidification in the Athabasca oil sands region, Alberta, Canada. Environ Sci Technol 2009;43(15):5844–50.

Whitfield CJ, Aherne J, Watmough SA, McDonald M. Estimating the sensitivity of forest soils to acid deposition in the Athabasca Oil Sands Region, Alberta. J Limnol 2010a; 69(1s):201–8. http://dx.doi.org/10.3274/JL10-69-S1-20.

Whitfield CJ, Aherne J, Cosby BJ, Watmough SA. Modelling catchment response to acid deposition: a regional dual application of the MAGIC model to soils and lakes in the Athabasca Oil Sands Region, Alberta. J Limnol 2010b;69(1s):147–60. http://dx.doi.org/10.3274/JL10-69- S1-15.

Whitfield CJ, Adkinson A, Eimers MC, Watmough SA. The adsorption and release of sulfur in mineral and organic soils of the Athabasca oil sands region, Alberta, Canada. J Environ Qual 2010c;39(3):1108–12.

Whitfield CJ, Watmough SA, Aherne J. Evaluation of elemental depletion weathering rate estimation methods on acid-sensitive soils of north-eastern Alberta, Canada. Geoderma 2011;166(1):189–97.

Whitfield CJ, Watmough SA. A regional approach for mineral soil weathering estimation and critical load assessment in boreal Saskatchewan, Canada. Sci Total Environ 2012;437:165–72.

Whitfield CJ, Reid C. Predicting surface area of coarse-textured soils: implications for weathering rates. Can J Soil Sci 2013;93(5):621–30.

Zhang XF. Atmospheric nitrogen wet deposition and its effects on wetland water environment of Shanghai area. Chin J Appl Ecol 2006;17:1099–102.